Received 27 November 2024, accepted 20 December 2024, date of publication 26 December 2024, date of current version 2 January 2025.

Digital Object Identifier 10.1109/ACCESS.2024.3522376

RESEARCH ARTICLE

Real-Time Duct Prediction and Propagation Analysis Using Genetic Algorithm-Based RFC and Parabolic Equation Method

JUN HEO[1], (Member, IEEE), DOYOUNG JANG[2], HOSUNG CHOO[3], (Senior Member, IEEE), DONG-YEOP NA[1], (Member, IEEE), AND YONG BAE PARK[4,5], (Senior Member, IEEE)

[1]Department of Electrical Engineering, Pohang University of Science and Technology, Pohang-si 37673, South Korea
[2]Radar System Team, Hanwha Systems, Yongin-si 17121, South Korea
[3]Department of Electronic and Electrical Engineering, Hongik University, Seoul 04066, South Korea
[4]Department of AI Convergence Network, Ajou University, Suwon-si 16499, South Korea
[5]Department of Electrical and Computer Engineering, Ajou University, Suwon-si 16499, South Korea

Corresponding author: Yong Bae Park (yong@ajou.ac.kr)

This work was supported in part by the Institute of Information and Communications Technology Planning and Evaluation (IITP), Korean Government (MSIT), Development of 3D-NET Core Technology for High-Mobility Vehicular Service under Grant 2022-0-00704-001; and in part by the Institute of Information and Communications Technology Planning and Evaluation (IITP), Korean Government (MSIT) under Grant RS-2024-00396992.

ABSTRACT This paper proposes a real-time prediction of the duct using a refractivity from clutter (RFC) method based on genetic algorithm (GA) and the parabolic equation (PE) method. Three dates with duct formation are selected, and the refractivity calculated using atmospheric measurements is compared with the refractivity obtained through the GA-based RFC method. Additionally, using the PE method, the electromagnetic wave propagation for each refractivity is analyzed and compared. The atmospheric refractivity and propagation prediction results derived from the proposed process are validated to be similar to those of the measurements. The proposed method enables real-time duct prediction and propagation trend analysis at low altitudes using clutter signals.

INDEX TERMS Duct prediction, genetic algorithm, parabolic equation method, propagation analysis, refractivity from clutter.

I. INTRODUCTION

The electromagnetic (EM) waves can travel long distances through the atmosphere, which varies in time and space, causing the waves to bend. In marine environments, atmospheric ducts can trap EM waves, enabling them to travel farther, leading to complex radar clutter signals and degraded radar performance. To predict EM wave propagation, calculating the atmospheric refractive index is essential, using measurements like atmospheric pressure, temperature, and water vapor. Traditional methods [1], [2], [3], [4], [5] accurately calculate this index but have limitations, particularly in marine environments, where land-based measurements are less reliable and cannot capture real-time atmospheric changes.

The associate editor coordinating the review of this manuscript and approving it for publication was Frederico Guimarães.

In long-range radar systems, the clutter power from the terrain or reflections on the sea surface can obstruct the interpretation of the signals. However, these clutter signals, influenced by atmospheric conditions such as ducts, can also be used to assess propagation in the duct case. This method, known as refractivity from clutter (RFC), estimates the low-altitude atmospheric state around the radar using only the clutter signals in the radar return, without temporal or spatial constraints. Thus, RFC is more suitable than traditional methods for evaluating atmospheres with propagation in the duct. Addressing the inverse problem of relating clutter signals to atmospheric refractive index, RFC requires algorithms to interpret this nonlinear relationship. Various methods have been attempted to implement the inversion algorithm. In [6], the inversion algorithm was implemented using a genetic algorithm (GA). The predicted data obtained through the GA-based method was then compared with data measured by a helicopter to verify its validity. In [7], refractivity tracking was implemented using both a Kalman filter and a particle filter, and the performance of each was verified and compared under various conditions. In [8], an inversion algorithm based on the particle swarm optimization method was proposed. In [9], an improved inversion algorithm was introduced by integrating particle swarm optimization with Lévy flight to improve performance over previous methods. In [10], a mapping method between sea clutter and refractivity profile using deep learning was proposed.

To analyze EM wave propagation using RFC, it is essential to apply numerical methods such as ray optics or the parabolic equation (PE) method [11], [12], [13], [14], [15]. Both of these methods are capable of handling long-range propagation scenarios that take into account varying atmospheric and boundary conditions. However, the PE method is often preferred for this type of analysis because it allows a more comprehensive quantitative assessment of propagation trends throughout an area. Although PE-based analyses of EM wave propagation are well-established [16], [17], [18], [19], [20], most previous studies have primarily focused on specific moments and localized environments. This leaves a gap in the research, especially for marine radar systems, where real-time atmospheric data is difficult to obtain. In such cases, a method that is independent of time and space for real-time propagation prediction becomes necessary, highlighting the need for further research.

In this paper, we propose a real-time prediction method of duct using a GA-based RFC method and the PE method. This method is designed to evaluate duct atmospheres and analyze the resulting EM wave propagation without being constrained by temporal or spatial limitations. The atmospheric refractivity predicted using our method is found to closely match actual atmospheric measurements, with the PE method confirming that the propagation trends align well between the predicted and observed data. Unlike traditional atmospheric measurement methods, which often suffer from significant time gaps between updates and lose accuracy with increasing distance from the measurement site, our approach facilitates real-time atmospheric assessment. By eliminating the need for direct measurements, this process overcomes temporal and spatial limitations, making it particularly well-suited for predicting duct propagation in marine environments, where immediate atmospheric assessment is both critical and challenging.

This paper is organized as follows: Section II describes the method for quantitatively modeling the atmosphere to calculate the refractivity, the method for calculating clutter power, and the implementation of the PE method for this purpose. Section III discusses the GA-based RFC process and the comparison between the results of the proposed process and the measured values. Section IV presents the conclusions.

II. MODELING OF CLUTTER SIGNAL AND PARABOLIC EQUATION METHOD

A. ATMOSPHERIC ENVIRONMENTS

In long-range environments, EM waves propagate through the troposphere, where atmospheric conditions such as pressure, temperature, and humidity vary with time and space. This variation contributes to the inhomogeneity of the atmosphere, the medium through which the waves travel, causing changes in the dielectric constant and resulting in the bending of the waves upwards or downwards. Thus, analyzing EM wave propagation in long-range environments requires considering the degree of refraction caused by the atmosphere. This is typically expressed using the atmospheric refractive index n or the refractivity N as shown in the following equation [21]:

$$n = \frac{c}{v} = \sqrt{\epsilon_r \mu_r} \tag{1}$$

$$N = (n-1) \times 10^6 = 77.6\frac{P}{T} + 3.73 \times 10^5 \frac{e}{T^2} \tag{2}$$

where c represents the speed of light in free space, v represents the phase velocity of the wave, ϵ_r and μ_r represent the relative permittivity and the relative permeability, respectively, P represents the pressure in $mbar$, T represents the absolute temperature in K, and e represents the partial pressure of water vapor in $mbar$.

Additionally, one important consideration in long-range environments is the assumption that the Earth is spherical, meaning it has a constant curvature. This assumption is crucial for accurately modeling how EM waves propagate over large distances. Therefore, it is convenient to transform the spherical domain of wave propagation analysis into a planar domain. The concept of modified refractivity facilitates this transformation by converting the spherical propagation problem over the curved Earth into a flat Earth scenario. This transformation allows for the use of Cartesian coordinates in calculations and intuitive interpretation of results. Refractivity can be replaced by modified refractivity for easier application, and for distances less than one-third of the Earth's radius, the transformation error is less than 1 % [22], [23]. The modified refractive index m, and the modified refractivity M can be calculated as follows [24]:

$$M = N + \frac{x}{a_e} \times 10^6 = N + 157x \tag{3}$$

$$m = M \times 10^{-6} + 1 \tag{4}$$

where x and a_e represent altitude and the Earth's radius, respectively.

In scenarios where EM waves propagate through the atmosphere without obstructions like reflection or shielding by terrain or sea surface, the propagation path is determined by the variation in refractivity with altitude. If the curvature of the propagation path is less than that of the Earth, the waves will tend to travel upward, a phenomenon known as sub-refraction. Conversely, if the curvature is greater, the waves will bend downward towards the Earth's surface, known as super-refraction. If the curvature increases significantly, causing the waves to refract enough to bounce off the surface, the waves appear to be trapped over certain regions, termed duct. These EM wave propagation paths are classified based on the change in refractivity with altitude.

Particularly, ducts form in layers of the atmosphere where the M decreases with altitude. This often occurs in maritime environments where dry air overlies moist air, leading to inversions of temperature or humidity. In such conditions, EM waves become trapped within the duct, potentially traveling much farther than typically expected. During such conditions, EM waves are more frequently exposed to surfaces such as the ground and the sea. As a result, there are increased reflections and radar may receive clutter signals from even more distant locations. Therefore, the radar returns containing clutter signals reflect the profile of altitude-dependent refractivity. By utilizing long-range maritime clutter, refractivity information can be obtained. Although clutter signals are generally weak or absent outside of duct conditions, the performance degradation of radar is mainly caused by such abnormal propagation within ducts, where clutter signals also increase in strength. Therefore, utilizing RFC allows for analysis of abnormal propagation in ducts.

B. RECEIVED CLUTTER POWER AND PARABOLIC EQUATION METHOD

Clutter power is derived as a function of environmental parameters and the radar signal. The power of EM waves received by the radar, when they hit a surface at a specific incidence angle from a distance r, is calculated as follows [22], [25], [26]:

$$P_r(r) = \frac{P_t G A_e \sigma F^4(r,m)}{(4\pi)^2 r^4 L_s} \tag{5}$$

where P_t represents the transmitted power, G represents the antenna gain, A_e represents the antenna effective aperture, σ represents the clutter cross section of the scatterer, L_s represents the total system losses, and $F(r, m)$ represents the propagation factor at the sea surface. The antenna effective aperture A_e can be expressed as a function of the wavelength λ and the antenna gain G as follows:

$$A_e = \frac{\lambda^2 G}{4\pi} \tag{6}$$

Additionally, the clutter cross section σ can be represented by the area of the radar cell A_c and the average clutter reflectivity factor per unit area σ_0 [26] as follows:

$$\sigma = A_c \sigma_0 \tag{7}$$

$$A_c = r\theta_B(c\tau/2)sec(\theta(r,m)) \tag{8}$$

where θ_B represents the azimuthal beamwidth, c represents the propagation speed, t represents the pulse width, and $\theta(r, m)$ represents the incidence angle. Therefore, the clutter power at a distance r is derived as follows:

$$P_c(r) = \frac{P_t G^2 \lambda^2 \theta_B c\tau \sigma_0 sec(\theta(r,m)) F^4(r,m)}{2(4\pi r)^3 L_s} \tag{9}$$

The average clutter reflectivity factor per unit area σ_0 is derived from empirical models created through experimental measurements. It varies between land and sea, and is calculated as follows [26], [27]:

$$\sigma_0(Land) = \frac{0.00032}{\lambda} \tag{10}$$

$$\sigma_0(Sea) = 10^{-6.4+0.6K_B+0.1sin\theta-0.1\lambda} \tag{11}$$

where θ represents the incidence angle, and K_B is the Beaufort wind scale number, which is a parameter used to determine the sea state based on wind speed [27]. As the incidence angle θ tends to vary inversely with distance. Therefore, in long-range environments, the θ becomes negligible. As a result, terms like $sec(\theta)$ or $sin(\theta)$, which are necessary for calculating clutter power, can almost be ignored. Consequently, clutter power can be normalized to the power at a range r_0, and can be expressed as follows:

$$\frac{P_c(r)}{P_c(r_0)} \approx \left(\frac{r_0}{r}\right)^3 \left(\frac{F(r,m)}{F(r_0,m)}\right)^4 \tag{12}$$

In long-range environments, the propagation factor $F(r, m)$ is a variable dependent on location and atmospheric conditions, making it a function of distance and refractivity. Calculation of $F(r, m)$ thus requires an analysis that considers the atmospheric refractivity over long distances. The PE method can be utilized for this purpose. The PE method is capable of handling two-dimensional EM wave problems involving longitudinal and transverse coordinates and is predominantly used for numerical analysis of tropospheric EM wave propagation.

The two-dimensional Helmholtz equation using distance z and altitude x can be expressed as follows [24]:

$$\nabla^2 U(z,x) + k_0^2 n^2 U(z,x) = 0 \tag{13}$$

where U represents the electric or magnetic field components in horizontal or vertical polarization, respectively, k_0 is the wavenumber of free space, and n means the refractive index of the medium. In addition, the two-dimensional scalar wave equation can be expressed as follows:

$$\frac{\partial^2 U(z,x)}{\partial z^2} + \frac{\partial^2 U(z,x)}{\partial x^2} + k_0^2 n^2 U(z,x) = 0 \tag{14}$$

In (13) and (14), it is assumed that the propagation medium is homogeneous, meaning that the refractive index n is the same across distances and altitudes. However, if changes in n are slow relative to the wavelength, it is possible to substitute n with $n(z, x)$ that changes with distance and altitude. The field component U can be expressed as a reduced function by separating the rapidly varying phase term. The field component U can then be represented as follows:

$$U(z,x) = e^{ik_0 z} u(z,x) \tag{15}$$

In this expression, $u(z, x)$ represents the amplitude of the wave, which changes slowly with distance and $e^{ik_0 z}$ is the phase term, which varies more rapidly. This formulation simplifies the analysis of EM wave propagation by focusing on the amplitude variations in the propagation direction.

In long-range environments, it can be assumed that EM waves propagate at very small angles relative to the horizon. In such cases, the paraxial approximation is applicable, and by substituting (15) into (14), the scalar wave equation for $u(z, x)$ can be expressed as follows [28]:

$$\left(\frac{\partial^2}{\partial x^2} + 2ik_0\frac{\partial}{\partial z} + k_0^2\left(n^2(z,x) - 1\right)\right)u(z,x) = 0 \quad (16)$$

The split step Fourier transform (SSFT) method is commonly used as an effective way to solve (16). This method is fast, easy to implement, and robust, making it suitable for analyzing EM wave propagation that accounts for the refractivity or terrain inhomogeneities within the analysis domain. The SSFT-based PE method considers only forward-propagating waves, ignoring any components that propagate in the opposite direction. Additionally, it is effective for analyzing waves emitted at small angles relative to the horizon.

The SSFT approach for PE divides the analysis domain into small distance segments. It uses the far field pattern of the antenna at distance zero to set the initial values. These initial values are then used to analyze the field profile for the next step of distance, and this process is repeated for each subsequent distance segment to derive the overall domain's EM wave propagation factors or path loss. Fourier transform is used to compute the field profile at a advanced distance $z + \Delta z$ from the profile at distance z. Typically, the fast Fourier transform (FFT) is implemented on computers for this purpose, and can be expressed as follows [14]:

$$u(z+\Delta z, x) = e^{(ik_0(n-1)\Delta z)} \times F^{-1}\left[e^{-ik_x^2\frac{\Delta z}{k_0+\sqrt{k_0^2-k_x^2}}} F(u(z,x))\right] \quad (17)$$

where F denotes the Fourier transform, and x and k_x are Fourier transform pairs. Here, $k_x = k_0 sin(\theta)$, where θ is the angle of EM wave propagation from the horizon. The refractive index n is used in (17), thus considering a scenario with a flat Earth as the boundary. Therefore, to incorporate Earth's curvature when using a spherical domain, n can be replaced with the modified refractive index m. The SSFT-based PE method requires that the analysis domain be divided in both distance and altitude directions. The intervals for distance Δz should be set larger than the wavelength, and the intervals for altitude Δx should be established according to the Nyquist sampling criterion as follows:

$$\Delta x \leq \frac{\lambda}{2sin(\theta_{max})} \quad (18)$$

where θ_{max} represents the maximum propagation angle. The results of the PE method are commonly represented by the distribution of field strength, typically expressed as path loss as follows [24]:

$$Loss(dB) = -20log_{10}u + 20log_{10}4\pi + 10log_{10}z - 30log_{10}\lambda \quad (19)$$

Additionally, path loss $L(r, m)$ can be transformed into the propagation factor $F(r, m)$ using the following equation:

$$F^2(r,m) = \left(\frac{4\pi r}{\lambda}\right)^2 / L(r,m) \quad (20)$$

By substituting (20) into (12), the path loss calculated using the PE method can be used to compute the normalized clutter power as follows:

$$\frac{P_c(r)}{P_c(r_0)} \approx \frac{r}{r_0}\left(\frac{L(r_0,m)}{L(r,m)}\right)^2 \quad (21)$$

III. PREDICTION OF REFRACTIVITY AND DUCT PROPAGATION

A. PROCESS OF GA COMBINED RFC METHOD

To predict duct propagation, it is necessary to assess the atmospheric environment. Typically, atmospheric information is collected to calculate refractivity and model the atmospheric conditions. However, such atmospheric information measurements are performed only two to four times a day at limited locations. This method of measurement poses temporal and spatial limitations when the radar is operated far from the measurement site, thereby making it challenging to predict duct propagation instantly. The RFC method is used to derive atmospheric refractivity inversely by utilizing clutter information continuously collected from the radar. This is based on the fact that the intensity of the clutter power spectrum is generally influenced by atmospheric conditions. For instance, during normal atmospheric conditions, the clutter intensity is observed to be relatively weak. In contrast, when a strong duct manifests, the impact of waves backscattered by the sea surface or ground increases, resulting in a strong clutter signal. Thus, by observing the intensity of the clutter, the atmospheric refractivity can be inversely deduced, allowing for the determination of duct propagation.

The Fig. 1 shows a trilinear model used in RFC methods for predicting atmospheric refractivity. The trilinear model represents the atmospheric refractivity with three lines (d_1, d_2, d_3) having different slopes based on altitude, with boundaries of each line defined from 0 m to h_1, h_2. The trilinear model is capable of modeling most atmospheric conditions, such as the general Earth's atmosphere, surface-based ducts, elevated ducts, and evaporation ducts, making it widely used input for analyzing EM wave propagation [29]. The variables d_1, d_2, d_3, h_1, and h_2 used in the trilinear model are used as parameters in the proposed RFC method.

The Fig. 2 illustrates the procedure of the GA used in the proposed RFC method. A GA is used to inversely predict atmospheric refractivity from the input clutter power spectrum. For this purpose, an arbitrary chromosome is first generated. The generated chromosome is restructured into five variables of the trilinear model, and the path loss for

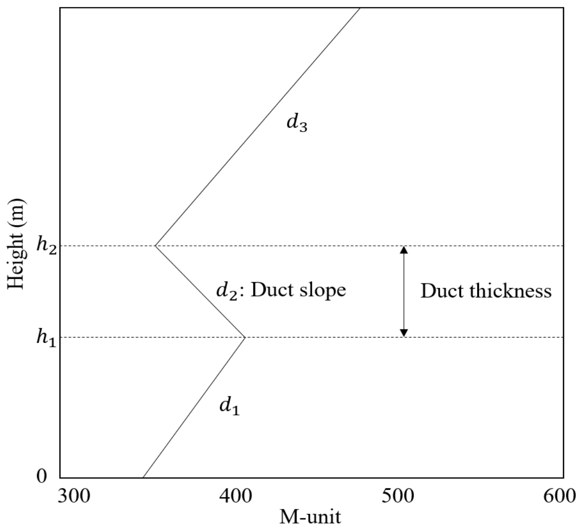

FIGURE 1. Trilinear modified refractivity model.

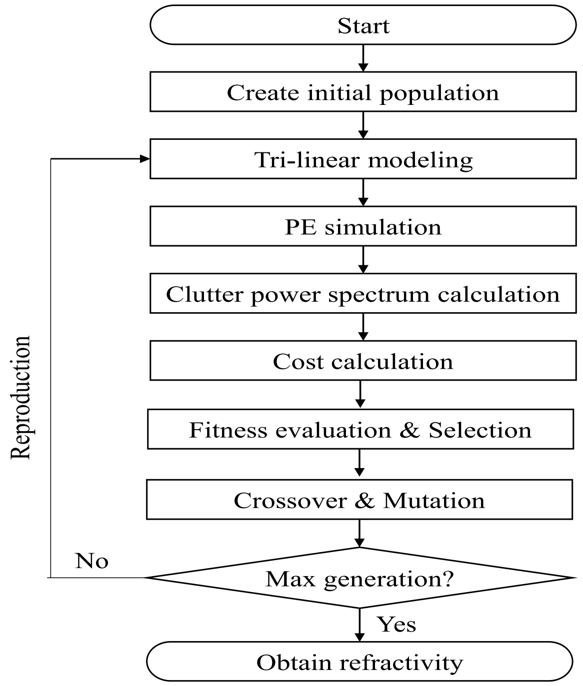

FIGURE 2. GA process for estimating atmospheric refractivity.

this atmospheric refractivity is obtained using the PE method. The calculated path loss and (21) are used to compute the clutter power spectrum, which is then compared to the input clutter power spectrum during the proposed RFC process. In this process, the fitness function is a key component, calculated as the difference between real and predicted clutter spectra, ensuring that a lower cost results in a higher fitness score. The GA follows a structured workflow involving chromosome encoding to represent the trilinear model variables, initial population generation for optimization, fitness evaluation for assessing solutions, and a selection mechanism to propagate favorable solutions to subsequent generations. The GA adjusts the trilinear model variables through a reconstruction process to minimize the difference between the two clutter power spectra, iteratively refining the model to achieve accurate spectral reconstruction. The GA parameters used in this prediction process are as follows in the Table 1. These parameters were selected through extensive experimentation to achieve an optimal balance between computational efficiency and prediction accuracy. A larger population size or increased number of generations could potentially improve convergence. However, such an approach would significantly increase computational time, making it impractical for real-world applications where atmospheric refractivity predictions are time-sensitive. This parameter configuration allows the GA to achieve reliable refractivity predictions within a short time, ensuring both reliability and operational feasibility.

TABLE 1. Detailed information of the GA.

Option	Value
Population size	30
Maximum generation	20
Elite count	6
Crossover ratio	40 %
Mutation ratio	10 %

B. NUMERICAL EXAMPLES AND DISCUSSION

To obtain the clutter power spectrum necessary for the RFC process, it is essential to calculate the path loss using the PE method and convert it into clutter power. The transmitting antenna is positioned at an arbitrary location, and path loss is calculated for a long-range area where the sea surface and low-altitude terrain, such as islands, are appropriately distributed. Such locations tend to show increased clutter signal strength when the atmosphere is in a strong duct state. The Fig. 3 illustrates the terrain distribution for the selected transmitting antenna location and the analysis area extending approximately 150 km.

FIGURE 3. Topographic map of the clutter power analysis area. Heuksan Island in South Korea, where the Tx is located, is a site where atmospheric measurements are performed.

Modeling the atmospheric refractivity required for path loss analysis is divided into four cases: no significant

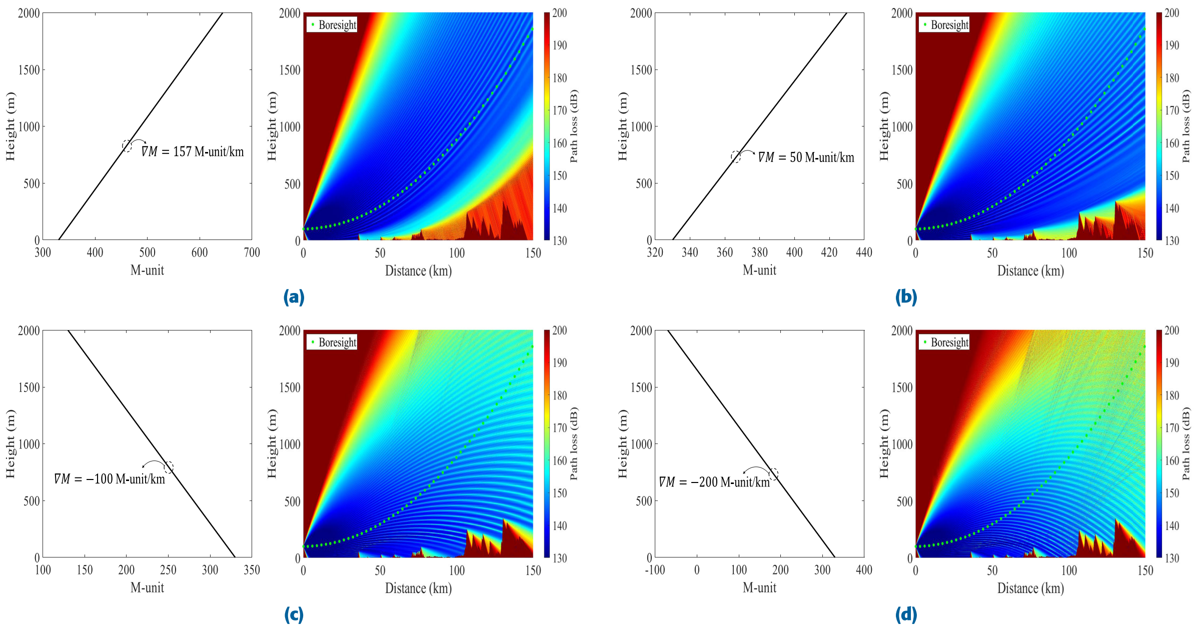

FIGURE 4. Atmospheric modified refractivity modelings and path loss distributions for each atmospheric condition. (a) Standard atmosphere with little to no refraction ($\nabla M = 157$), (b) Atmosphere with partial downward refraction ($\nabla M = 50$), (c) Atmosphere in a duct state ($\nabla M = -100$), and (d) Atmosphere in a strong duct state ($\nabla M = -200$).

refraction of EM waves ($\nabla M = 157$), slight refraction below the boresight ($\nabla M = 50$), duct state ($\nabla M = -100$), and strong duct state ($\nabla M = -200$). The transmitting antenna is positioned at an altitude of 100 m, with a 3 dB beamwidth of 1°, an elevation angle of 0°, and a frequency of 3 GHz. The path loss distribution for each atmospheric modeling is shown in the Fig. 4. The green dotted line represents the boresight of the antenna, and because the spherical Earth is transformed into a planar one, it appears curved due to the transformation.

In a standard atmospheric state ($\nabla M = 157$), EM waves propagate mostly through the air. Due to the low altitude of the terrain in the analysis area, there are few obstacles to scatter the propagating EM waves. As shown in Fig. 4(a), the path loss distribution is only affected by the terrain located approximately 35 km away, with almost no impact on the remaining distance interval. Therefore, the clutter power spectrum received by the radar tends to decrease in intensity as the distance increases. In the atmospheric state of $\nabla M = 50$, where EM waves bend downward below the antenna boresight, as shown in Fig. 4(b), EM waves are not directly affected by the sea surface yet. Instead, they are partially obstructed by some terrain. In this case, additional backscattered components occur, leading to an increase in the clutter power. In the duct state of $\nabla M = -100$ and the strong duct state of $\nabla M = -200$, where EM waves bend completely towards the surface, EM waves are significantly refracted downward and are greatly affected by the sea surface and terrain. In these duct propagation environments, many backscattered wave components are generated, resulting in an increase in the clutter power spectrum in some regions. The path loss distribution in Fig. 4(c) and 4(d) predicts that backscattered wave components will occur due to both the

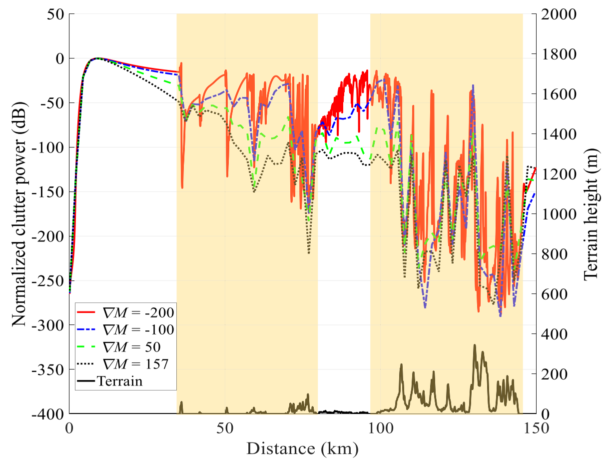

FIGURE 5. Normalized clutter power distribution for the four cases.

sea surface and the terrain. Especially in Fig. 4(d), it can be predicted that the EM waves will be refracted even more strongly downward, resulting in stronger clutter power being received.

The normalized clutter power distribution at a low altitude near the sea surface for the four cases can be represented as shown in Fig. 5. In the atmospheric state with $\nabla M = 157$, where the impact of the sea surface and terrain is minimal, a general result is obtained, showing a tendency for clutter power to decrease with distance. In the atmospheric state with $\nabla M = 50$, the clutter power distribution shows an increase compared to the previous result due to the influence of the terrain located 35 km away. Similarly, beyond 100 km, there are few obstacles to cause interference, showing only a slight difference. In the duct scenarios ($\nabla M = -100, -200$),

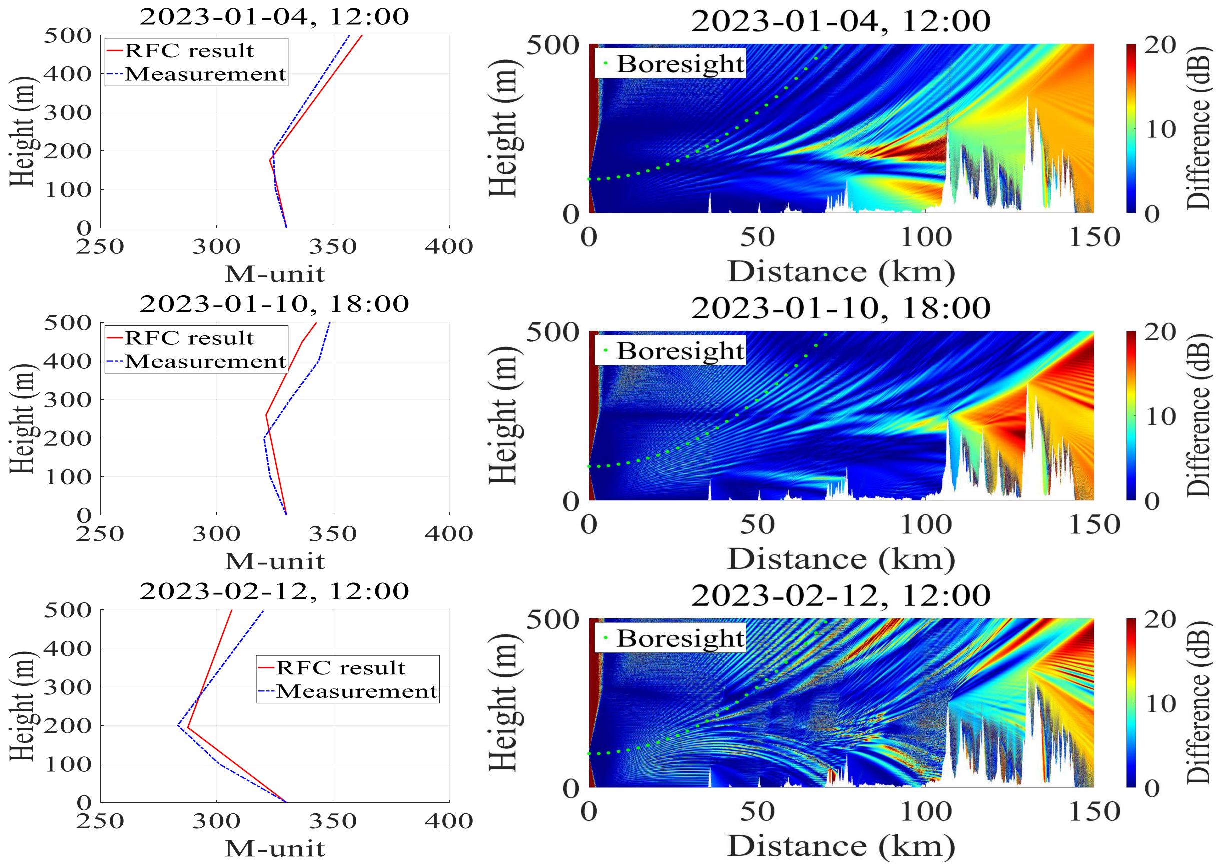

FIGURE 6. **Comparison of refractivity on three dates derived from measurements and the RFC method.**

clutter power is significantly stronger compared to the general atmosphere. Particularly in the regions affected by terrain and the sea surface between them, the clutter power distribution has an overall strong intensity. Although the difference is small, the atmospheric state with $\nabla M = -200$, where refraction is more severe, shows slightly stronger clutter power. Thus, in duct propagation, high-intensity clutter power is typically observed by radar, and using this information with the RFC method allows for predicting atmospheric conditions without atmospheric environment measurements.

The path loss derivation using the PE method and the clutter power spectrum calculation process can be used as inputs for the GA-based RFC method. The prediction results of the atmospheric modified refractivity derived using the proposed RFC method are shown in Fig. 6 and are compared with measurements from Heuksan Island, South Korea, where the transmitting antenna is located. The atmospheric observations, conducted 2 to 4 times daily, provide pressure, temperature, and water vapor pressure at various altitudes, which can be used to calculate atmospheric refractivity using 2. Among the many measurement data, three dates with duct formation are selected and compared with the refractivity results derived by the RFC method. Since the clutter power is formed by backscattered wave components generated at low altitudes, the analysis is limited to results up to an altitude of 500 m, where the prediction accuracy is limited at higher altitudes. atmospheric measurements have the limitation of potentially not acquiring new data for up to 12 hours. Since changes in atmospheric refractivity do not occur rapidly in real environments, this method is deemed a suitable method for predicting duct propagation in marine environments, which are far from atmospheric observation stations and where immediate atmospheric assessment is challenging.

Examining the modified refractivity distribution for the three selected dates with duct formation, a surface duct is observed on all dates, with a negative gradient from an altitude of 0 m to a certain height. For propagation analysis under such atmospheric conditions, it is important to predict the gradient of the modified refractivity and the altitude where the gradient shifts from negative to positive. For all three dates, the refractivity predicted using the RFC method appropriately estimated the altitude and gradient of the duct layer when compared with the measurements.

Using the PE method, EM wave propagation is analyzed on these three dates, comparing actual atmospheric observations with RFC-derived results, utilizing a Gaussian antenna located at an altitude of 100 m and operating at a frequency of 3 GHz. The differences are shown in the right side of Fig. 1. The differences between observation and RFC results

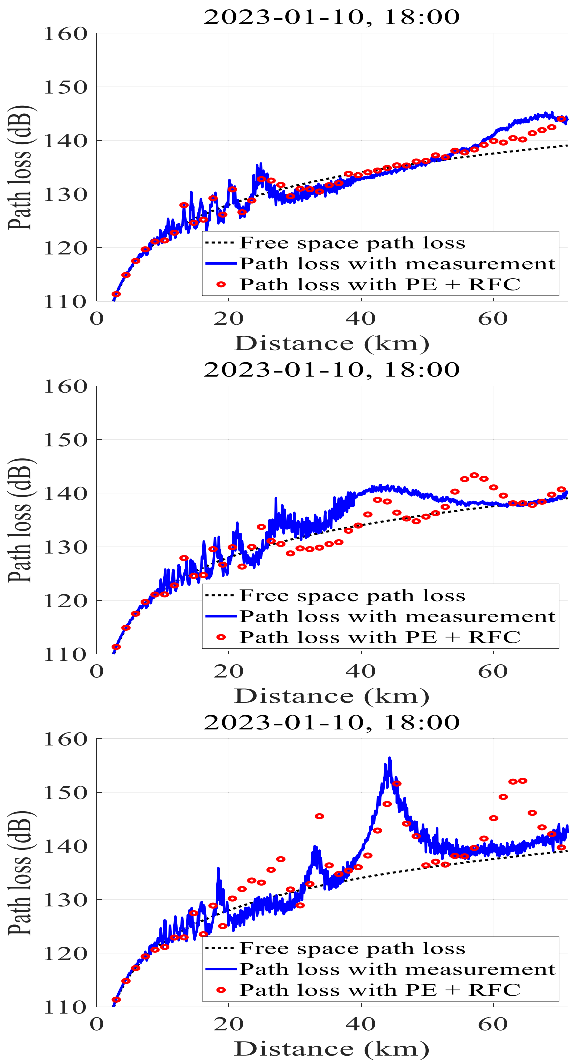

FIGURE 7. Path loss prediction results in the antenna boresight direction for three dates.

are minimal but show some divergence beyond 100 km due to terrain obstructions. These discrepancies are likely due to slight differences between observed values and RFC predictions, which affect terrain interaction. Overall, the RFC method provides a close approximation to actual EM wave propagation under duct conditions.

Additionally, since it is necessary to predict the impact of duct propagation in the direction the antenna is pointing, path loss analysis is performed in the antenna boresight direction based on atmospheric measurements and the RFC method. Fig. 7 shows the path loss calculated in the antenna boresight direction for three dates with duct conditions, compared to free-space path loss. Due to the occurrence of duct propagation, EM waves tend to direct towards the surface, increasing the effects of multipath fading. As a result, the overall trend is similar to free-space path loss, but fluctuations appear in the path loss distribution. It can be confirmed that the path loss distribution analyzed using measurements and the results analyzed using the proposed method correlate closely.

In summary, by referencing data from actual atmospheric observation sites, three dates with duct conditions are identified. The atmospheric refractivity derived from atmospheric observation values is compared with that obtained using GA-based RFC, and the duct propagation prediction performance is verified. The proposed method is found to match well with the measurements. Actual atmospheric observations can take between 6 to 12 hours to receive new data and have spatial and temporal limitations, which are valid only at the measurement site. However, the proposed method has been shown to provide new information more quickly and accurately predict duct propagation.

IV. CONCLUSION

In this paper, a real-time duct propagation prediction process using the parabolic equation method and a genetic algorithm (GA)-based refractivity from clutter (RFC) method is proposed. To validate the proposed method, atmospheric observation data from Heuksan Island in South Korea are referenced, specifically selecting dates when duct propagation is present. The atmospheric refractivity derived from atmospheric observation is compared with that obtained using the GA-based RFC method for three dates with surface ducts. It is confirmed that the height of the duct layer and the gradient of refractivity with altitude are well predicted. Additionally, using the predicted atmospheric refractivity, the propagation analysis is performed. By comparing the results, it is verified that the proposed process aligns closely with the measurements.

Traditional measurement methods have the limitation of data gaps for 6 to 12 hours and become less reliable as the distance from the measurement site increases. However, the proposed method can acquire valid data wherever radar clutter power is available, overcoming temporal and spatial limitations. The proposed process can be applied for real-time duct propagation prediction in marine environments that are far from atmospheric observation stations and where immediate atmospheric assessment is challenging.

REFERENCES

[1] J. J. Sylvester, G. C. Konstanzer, J. R. Rottier, G. D. Dockery, and J. Rowland, "Aegis anti-air warfare tactical decision aids," *Johns Hopkins APL Tech. Dig.*, vol. 22, no. 4, pp. 473–487, Jan. 2001.

[2] R. M. Hodur, "The naval research laboratory's coupled ocean/atmosphere mesoscale prediction system (COAMPS)," *Monthly Weather Rev.*, vol. 125, no. 7, pp. 1414–1430, 1997.

[3] E. R. Thews, "Timely prediction of low-altitude radar performance in operational environments using *in situ* atmospheric refractivity data," in *IEE Proceedings F* (Radar and Signal Processing), vol. 137. Edison, NJ, USA: IET, 1990, pp. 89–94.

[4] R. Douvenot, V. Fabbro, P. Gerstoft, C. Bourlier, and J. Saillard, "A duct mapping method using least squares support vector machines," *Radio Sci.*, vol. 43, no. 6, pp. 1–12, Dec. 2008.

[5] B. W. Atkinson, J.-G. Li, and R. S. Plant, "Numerical modeling of the propagation environment in the atmospheric boundary layer over the Persian Gulf," *J. Appl. Meteorol.*, vol. 40, no. 3, pp. 586–603, Mar. 2001.

[6] P. Gerstoft, L. T. Rogers, J. L. Krolik, and W. S. Hodgkiss, "Inversion for refractivity parameters from radar sea clutter," *Radio Sci.*, vol. 38, no. 3, pp. 18-1–18-22, Jun. 2003.

[7] C. Yardim, P. Gerstoft, and W. S. Hodgkiss, "Tracking refractivity from clutter using Kalman and particle filters," *IEEE Trans. Antennas Propag.*, vol. 56, no. 4, pp. 1058–1070, Apr. 2008.

[8] B. Wang, Z.-S. Wu, Z. Zhao, and H.-G. Wang, "Retrieving evaporation duct heights from radar sea clutter using particle swarm optimization (PSO) algorithm," *Prog. Electromagn. Res. M*, vol. 9, pp. 79–91, 2009.

[9] Z.-H. Zhang, Z. Sheng, and H.-Q. Shi, "Parameter estimation of atmospheric refractivity from radar clutter using the particle swarm optimization via Lévy flight," *J. Appl. Remote Sens.*, vol. 9, no. 1, Oct. 2015, Art. no. 095998.

[10] X. Guo, J. Wu, J. Zhang, and J. Han, "Deep learning for solving inversion problem of atmospheric refractivity estimation," *Sustain. Cities Soc.*, vol. 43, pp. 524–531, Nov. 2018.

[11] L. Sevgi and L. B. Felsen, "A new algorithm for ground wave propagation based on a hybrid ray-mode approach," *Int. J. Numer. Modelling, Electron. Netw., Devices Fields*, vol. 11, no. 2, pp. 87–103, Mar. 1998.

[12] L. Sevgi, "A ray-shooting visualization MATLAB package for 2D groundwave propagation simulations," *IEEE Antennas Propag. Mag.*, vol. 46, no. 4, pp. 140–145, Aug. 2004.

[13] L. Sevgi, "Groundwave modeling and simulation strategies and path loss prediction virtual tools," *IEEE Trans. Antennas Propag.*, vol. 55, no. 6, pp. 1591–1598, Jun. 2007.

[14] G. Apaydin and L. Sevgi, *Radio Wave Propagation and Parabolic Equation Modeling*. Hoboken, NJ, USA: Wiley, 2017.

[15] P. Zhang, L. Bai, Z. Wu, and L. Guo, "Applying the parabolic equation to tropospheric groundwave propagation: A review of recent achievements and significant milestones," *IEEE Antennas Propag. Mag.*, vol. 58, no. 3, pp. 31–44, Jun. 2016.

[16] X.-M. Guo, Q.-L. Li, Q. Zhao, S.-F. Kang, Y.-W. Wei, and L.-X. Yang, "A comparative study of rough sea surface and evaporation duct models on radio wave propagation," *IEEE Trans. Antennas Propag.*, vol. 71, no. 7, pp. 6060–6071, Jul. 2023.

[17] X. Cao, J. Liu, J. Hao, Q. Zhao, B. Xue, F. Zhang, J. Fan, C. Lin, and Z. Dong, "Modeling analysis and research of terahertz wave propagation experiment at sea," *IEEE Trans. THz Sci. Technol.*, vol. 14, no. 3, pp. 377–385, May 2024.

[18] H. Yu, C. Liao, J. Feng, W. Du, and X. Zhong, "Analysis of radar target scattering echo with surface ducting in large-scale environments based on the PE-MoM hybrid method," *IEEE Antennas Wireless Propag. Lett.*, vol. 22, no. 9, pp. 2295–2299, Sep. 2023.

[19] B. Shu, W. Zhang, Y. He, J. Sun, and C.-X. Wang, "Application of ray tracing for beyond-line-of-sight maritime communication in evaporation ducts," in *Proc. Int. Wireless Commun. Mobile Comput. (IWCMC)*, Jun. 2023, pp. 1034–1039.

[20] Q. Zhang, S. Wang, Y. Shi, and K. Yang, "Measurements and analysis of maritime wireless channel at 8 GHz in the South China Sea region," *IEEE Trans. Antennas Propag.*, vol. 71, no. 3, pp. 2674–2681, Mar. 2023.

[21] *The Radio Refractive Index: Its Formula and Refractivity Data*, document Rec. ITU-R P. 453-14, 2019.

[22] A. Karimian, C. Yardim, P. Gerstoft, W. S. Hodgkiss, and A. E. Barrios, "Refractivity estimation from sea clutter: An invited review," *Radio Sci.*, vol. 46, no. 6, pp. 1–16, Dec. 2011.

[23] C. L. Pekeris, "Accuracy of the earth-flattening approximation in the theory of microwave propagation," *Phys. Rev.*, vol. 70, nos. 7–8, pp. 518–522, Oct. 1946.

[24] M. Levy, *Parabolic Equation Methods for Electromagnetic Wave Propagation*, no. 45. Edison, NJ, USA: IET, 2000.

[25] G. D. Dockery, "Method for modelling sea surface clutter in complicated propagation environments," in *IEE Proceedings F* (Radar and Signal Processing), vol. 137. Edison, NJ, USA: IET, 1990, pp. 73–79.

[26] M. I. Skolnik, *Radar Handbook*, 3rd ed. New York, NY, USA: McGraw-Hill, 2008.

[27] D. K. Barton, *Radar Equations for Modern Radar*. Norwood, MA, USA: Artech House, 2013.

[28] J. R. Kuttler and G. D. Dockery, "Theoretical description of the parabolic approximation/Fourier split-step method of representing electromagnetic propagation in the troposphere," *Radio Sci.*, vol. 26, no. 2, pp. 381–393, Mar. 1991.

[29] S. Vasudevan, R. H. Anderson, S. Kraut, P. Gerstoft, L. T. Rogers, and J. L. Krolik, "Recursive Bayesian electromagnetic refractivity estimation from radar sea clutter," *Radio Sci.*, vol. 42, no. 2, pp. 1–19, Apr. 2007.

JUN HEO (Member, IEEE) received the B.S. and Ph.D. degrees in electrical and computer engineering from Ajou University, South Korea, in 2018 and 2024, respectively. Since 2024, he has been working as a Postdoctoral Researcher with Pohang University of Science and Technology (POSTECH), South Korea. His research interests include tropospheric electromagnetic wave propagation, radar performance analysis, and wireless power transfer.

DOYOUNG JANG received the B.S. degree in information and telecommunication engineering from Dongyang Mirae University, Seoul, Republic of Korea, in 2018, and the M.S. and Ph.D. degrees in electronic and electrical engineering from Hongik University, Seoul, in 2020 and 2023, respectively. He worked as a Research Engineer at MOASOFT, Seoul, from 2015 to 2018, and from 2023 to 2024, he worked as a Research Professor at the Metamaterial Electronic Component Research Center, Hongik University. He currently joined Hanwha Systems as a Senior Engineer. His research interests include array antennas, radars, and electromagnetic wave propagation.

HOSUNG CHOO (Senior Member, IEEE) received the B.S. degree in radio science and engineering from Hanyang University, Seoul, in 1998, and the M.S. and Ph.D. degrees in electrical and computer engineering from The University of Texas at Austin, in 2000 and 2003, respectively. In September 2003, he joined the Department of Electronic and Electrical Engineering, Hongik University, Seoul, South Korea, where he is currently working as a Professor. His principal area of research interests include electrically small antennas for wireless communications, reader, and tag antennas for RFID, on-glass and conformal antennas for vehicles and aircraft, and array antennas for GPS applications.

DONG-YEOP NA (Member, IEEE) received the B.S. and M.S. degrees in electrical and computer engineering from Ajou University, Suwon-si, South Korea, in 2012 and 2014, respectively, and Ph.D. degree in electrical and computer engineering from The Ohio State University, Columbus, OH, USA, in 2018. From 2019 to 2022, he was at the Elmore Family School of Electrical and Computer Engineering, Purdue University, West Lafayette, IN, USA, as a Postdoctoral Research Associate and a Research Scientist. He joined the Department of Electrical Engineering, Pohang University of Science and Technology, Pohang-si, South Korea, in 2022, where he is currently working as an Assistant Professor. His research interests include computational electromagnetics, kinetic plasma modeling via particle-in-cell algorithm, and quantum electromagnetics.

YONG BAE PARK (Senior Member, IEEE) received the B.S., M.S., and Ph.D. degrees in electrical engineering from the Korea Advanced Institute of Science and Technology, South Korea, in 1998, 2000, and 2003, respectively. From 2003 to 2006, he was at Korea Telecom Laboratory, Seoul, South Korea. He joined the School of Electrical and Computer Engineering, Ajou University, South Korea, in 2006, where he is currently working as a Professor. His research interests include electromagnetic field analysis, high-frequency methods, metamaterial antennas, radomes, and stealth technology.